https://doi.org/10.21289/KSIC.2020.23.2.115 KSIC

Wireless Power Transfer for Electric Vehicles Charging Based on Hybrid Topology Switching With a Single Inverter

Yafei Chen[1], Hailong Zhang[2], Dong-Hee Kim[3], Sung-Jun Park[4], Seong-Mi Park[5*]

〈Abstract〉

In wireless power transfer (WPT) system, the conventional compensation topologies only can provide a constant current (CC) or constant voltage (CV) output under their resonant conditions. It is difficult to meet the CC and CV hybrid charging requirements without any other schemes. In this study, a switching hybrid topology (SHT) is proposed for CC and CV electric vehicle (EV) battery charging. By utilizing an additional capacitor and two AC switches (ACSs), a double-side LCC (DS-LCC) and an inductor and double capacitors-series (LCC-S) topologies are combined. According to the specified CC and CV charging profile, the CC and CV charging modes can be flexibly converted by the two additional ACSs. In addition, zero phase angle (ZPA) also can be achieved in both charging modes. In this method, because the operating frequency is fixed, without using PWM control, and only a small number of devices are added, it has the benefits of low-cost, easy-controllability and high efficiency. A 3.3-kW experimental prototype is configured to verify the proposed switching hybrid charger. The maximum DC efficiencies (at 3.3-kW) of the proposed SHT is 92.58%.

Keywords : Wireless power transfer (WPT), Constant current&voltage (CC&CV) charging, Electric vehicle (EV), Double-side LCC (DS-LCC), inductor and double capacitors-series (LCC-S), Zero phase amgle (ZPA).

1 Main Author, Ph.D. Course, Dept. of Electrical Engineering, Chonnam National University
E-mail: swjtuqust@163.com
2 Author, Ph.D. Course, Dept. of Electrical Engineering, Chonnam National University
E-mail: hailong9925@gmail.com
3 Author, Dept. Electrical Engineering, Chonnam National University, Assistant Professor.
E-mail: kimdonghee@chonnam.ac.kr
4 Author, Dept. Electrical Engineering, Chonnam National University, Professor.
E-mail: sjpark1@jnu.ac.kr
5* Corresponding Author, Dept. of Lift Engineering, Korea Lift College, Associate Professor.
E-mail: seongmi@klc.ac.kr

1. Introduce

Electric vehicle (EV) battery charging methods include contact charging and wireless charging [1], [2]. Compared with contact charging, wireless charging has the advantages of no contact loss, no mechanical wear, safety, and reliability [3]-[4]. Thus, wireless charging has received increasing attention.

EV battery charging has several charging strategies, e.g., CC charging, CV charging and CC/CV hybrid charging [5]. According to the characteristics of battery, and combining the advantages of CC and CV charging. Generally, CC/CV hybrid charging is widely utilized in EV industrial [6]. The typical profile of CC/CV hybrid charging is shown in Fig. 1. The entire charging process is divided into two stages, which are CC mode and CV mode. In CC mode, the charging current is constant and charging voltage gradually increases. The CV mode begins when the charging voltage increases to specified voltage, the charging voltage remains unchanged and the charging current slowly decreases until zero. The equivalent resistance continues to rise throughout the entire charging process.

In wireless power transfer (WPT) system, normally, two conventional methods are often used to realize CC and CV hybrid charging. First, by adding an additional DC-DC converter behind the secondary rectifier and using PI control method to regulate the

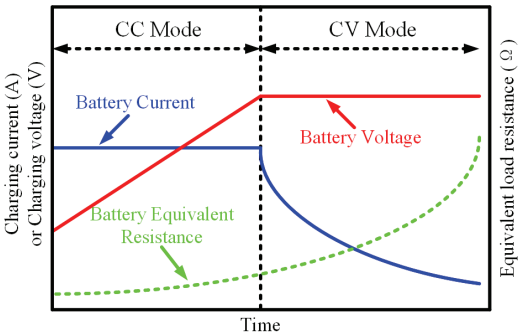

Fig. 1 Typical profile of EV battery charging

outputs directly [7], however, this method increases the cost and volume of the whole WPT system, and lower the total systeme efficiency. Another method is using phase-shift (PS) and frequency modulation (FM) hybrid control to adjust the effective input voltage [8]. Even though the outputs can be indirectly regulated, the operating frequency should be continuously changed to satisfy the zero voltage switching (ZVS) condition, thus, the control process is very complex, and the DC-link voltage utilization is low.

In order to achieve the CC and CV outputs for hybrid battery charging and ZPA for high efficiency, simultaneously. In WPT system, the numerous compensation topologies which have a CC/CV output can be reconfigured and combined by using ACSs. In this method, because the operating frequency is fixed, without using PWM control and only a small number of devices are required, it attracts increasing attentions of researchers. In [9], a composite topology, which combines a series-series (S-S) and a series-parallel (SP) topology, was proposed.

CC and CV output can be realized by switching; however, because a center-tapped transformer and three ACSs are required, the topology sturcture is complex. In [10], a switching hybrid LCC-S compensation topology was proposed. Based on a conventional LCC-S topology, two additional capacitors were added to the topology for the implementation of CC and ZPA, and CC and CV charging modes can be converted by using two ACSs, however, the two ACSs were placed in both primary and secondary sides, therefore, wireless communication is required for synchronous control. In this study, an SHT is proposed for CC and CV hybrid charging, the combination of a DS-LCC and a LCC-S topologies can be implemented only through an additional capacitor and two ACSs. In addition, all the additional resonant devices are plaeced in the secondary side, thus, the battery information can be directly obtained by the secondary controller, and wireless communication is not needed. A 3-kW experimental prototype is configured, and comparative experiments are conducted to verify the proposed SHT.

2. Theoretical Analysis

2.1 Fundamental Analysis of the WPT system

Fig. 2 shows the structure of the proposed WPT system based on SHT. U_{DC} is the DC-link voltage. A full-bridge inverter (FBI) is applied to convert the DC components into AC components. U_{AB} and I_{IN} are the output voltage and current of the FBI, respectively. If U_{AB} is expanded by the Fourier series, it can be expressed as

$$U_{AB}=\frac{4U_{DC}}{\pi}\sum_{n=1,3,5...}\frac{\sin(n\phi)}{n} \quad (1)$$

where n is the number of harmonics and φ is the phase angle. S_1 and S_2 are the corresponding ACSs to switch the CC and CV charging modes. The bridge rectifier (BR) is

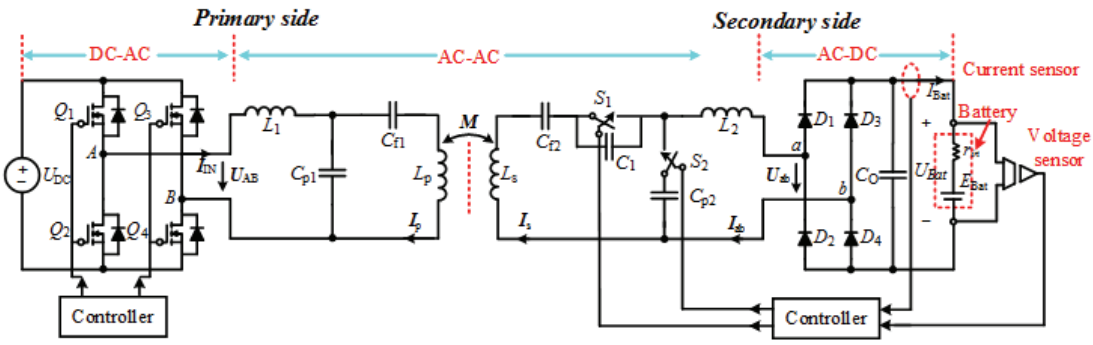

Fig. 2 WPT system based on proposed switching hybrid compensation topology

(a) (b)

Fig. 3 Equivalent models of loosely coupled transformer. (a) M model. (b) T model.

applied to transform the AC output voltage $\dot{U}_{ab}$ and current $\dot{I}_{ab}$ to battery charging voltage U_{Bat} and current I_{Bat}, respectively. While the fundamental harmonic analysis (FHA) method is utilized to analyze, and the output low-pass filter (LPF) consists only of the capacitance C_O, the following equations can be derived according to [11]:

$$\begin{cases} U_{Bat} = \dfrac{\pi\sqrt{2}}{4} U_{ab} \\ I_{Bat} = \dfrac{2\sqrt{2}}{\pi} I_{ab} \\ R_{Bat} = \dfrac{\pi^2}{8} R_{Ac} \end{cases} \tag{2}$$

where U_{ab} and I_{ab} are the RMS values of $\dot{U}_{ab}$ and $\dot{I}_{ab}$. The output AC and DC equivalent resistance are defined as R_{Ac} = U_{ab} / I_S, and R_{Bat} = U_{Bat} / I_{Bat}, respectively.

In WPT system, the loosely coupled transformer (LCT) is a key component, Generally, there are two analytical models utilized to analyze LCT, which are named M model and T model, as shown in Fig. 3. L_p and L_s are the self-inductances of primary coil and secondary coil, respectively. M is the mutual inductance of LCT. On the premise that the M model and the T model are equivalent, and the following equations can be derived

$$\begin{cases} L_T = L_p - M \\ L_R = L_s - M \end{cases} \tag{3}$$

where L_T and L_R are the leakage inductance of the primary coil and secondary coil when the turn ratio is same.

2.2 CV Mode Analysis of the Proposed Switching Hybrid Compensation Topology

In Figure 2, if the ACSs S_1 and S_2 both off, the equivalent T model for CC mode can be shown in Fig. 4(a). If the series-connections of L_R and L_2 are considered as a whole inductor L', while the series-connections of C_1 and C_{f2} are considered as a whole capacitor C', there are

$$\begin{cases} L' = L_R + L_2 \\ C' = \dfrac{C_1 C_{f2}}{C_1 + C_{f2}} \end{cases} \tag{4}$$

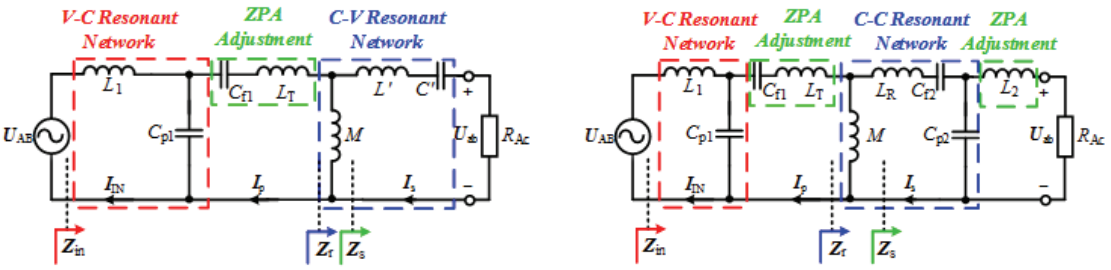

Fig. 4 Equivalent T models of the proposed switching hybrid compensation topology (a) for CV mode. (b) for CC mode

when C' is large enough, the series-connection of L' and C' can be regarded as an equivalent capacitance C_0, i.e.,

$$C_0 = \frac{C'}{1-\omega_0^2 L' C'} \tag{5}$$

The angular frequency of U_{AB} is defined as ω_0 and is referred to as the operation angular frequency of the resonant network hereafter. In the V-C resonant network, when L_1 resonate with C_{p1}, i.e., $\omega_0^2 = 1 / (L_1 C_{p1})$, the primary coil current I_p can be obtained as

$$I_p = \frac{U_{AB}}{j\omega_0 L_1} \tag{6}$$

The RMS value of I_p is a constant and is irrelevant to the other parameters of the topology. In the C-V resonant network, when M resonate with C_0, i.e., $\omega_0^2 = 1 / (MC_0)$, and by combining (2) the battery charging voltage U_{Bat} can be derived as

$$U_{Bat} = \frac{\pi\sqrt{2} M U_{AB}}{4 L_1} \tag{7}$$

From (7), it can be seen that the battery charging voltage U_{Bat} is constant and independent of load in CV mode. In Fig. 3(a), the total input impedance Z_{in} can be given as

$$Z_{\in} = \left[\left(j\omega_0 L_T + \frac{1}{j\omega_0 C_{f1}} + (j\omega_0 M // Z_s)\right) // \frac{1}{j\omega_0 C_{p1}}\right] + j\omega_0 L_1 \tag{8}$$

Under the condition of $\omega_0^2 = 1 / (L_1 C_{p1}) = 1 / (MC_0)$, and substituting (3) into (8), the condition to implement ZPA can be derived as

$$L_1 = \left(\frac{C_{f1}}{C_{f1} + C_{p1}}\right) L_p \tag{9}$$

Under the condition as given in (9), and combining (2), the input impedance of ZPA in CV mode can be given as

$$Z_{\in} = \frac{8}{\pi^2} \frac{L_1^2 R_{Bat}}{M^2} \tag{10}$$

2.3 CC Mode Analysis of the Proposed Switching Hybrid Compensation Topology

In Figure 2, if the ACSs S_1 and S_2 both on, the equivalent T model for CC mode can be shown in Fig. 4(b). If L_T and L_R are much larger than C_{f1} and C_{f2}, their series-connections can be considered as two equivalent inductors L_T' and L_R', i.e.,

$$\begin{cases} L_T' = L_T - \dfrac{1}{\omega_0^2 C_{f1}} \\ L_R' = L_R - \dfrac{1}{\omega_0^2 C_{f2}} \end{cases} \tag{11}$$

When L_1 resonate with C_{p1}, the primary coil current I_p is same with that in CV mode. If the C-C resonant network operates under its resonant condition, i.e.,

$$\omega_0^2 = \frac{1}{L_R' C_{p2} + M C_{p2}} \tag{12}$$

Thus, the AC output current I_{ab} can be derived as

$$I_{ab} = \frac{M}{L_R' + M} I_p = \frac{M U_{AB}}{j\omega_0 L_1 L_2} \tag{13}$$

by substituting (2) to (13), the battery charging current I_{Bat} can be derived as

$$I_{Bat} = \frac{2\sqrt{2} M U_{AB}}{\pi \omega_0 L_1 L_2} \tag{14}$$

From (14), it can be seen that the battery charging voltage I_{Bat} is constant and independent of load in CC mode. From Fig. 3(b) and according to the previous analysis, the total input impedance Z_{in} in CC mode can be expressed as (8). To realize ZPA in CC mode, the following equations should be satisfied

$$\omega_0^2 (L_p - L_1) C_{f1} = \omega_0^2 (L_s - L_2) C_{f2} = 1 \tag{15}$$

Under the condition as given in (15), and combining (2), the input impedance of ZPA in CC mode can be given as

$$Z_{in} = \frac{8}{\pi^2} \frac{\omega_0^2 L_1^2 L_2^2}{R_{Bat} M^2} \tag{16}$$

2.4 Parameter Modification-based CC and CV Mode Implementation for WPT system

For the proposed switching hybrid compensation topology, the parameter design method for CC/CV output implementation is produced in detail below. Under the condition that LCT parameters have been given, the parameters of the proposed switching hybrid compensation topology are designed according to the specified CC and CV values. Because the primary side compensation devices are shared in both CC and CV charging modes, and the circuit in CV mode is more simple than that in CC

mode, the primary side devices should be determined according to Fig. 4(a). Under the resonant condition and according to (7), primary compensation inductance L_1 can be designed as

$$L_1 = \frac{\pi\sqrt{2}MU_{AB}}{4L_1U_{Bat}} \tag{17}$$

After the determination of L_1, the primary compensation capacitances C_{p1} and C_{f1} can be determined as

$$\begin{cases} C_{p1} = \dfrac{1}{\omega_0^2 L_1} \\ C_{f1} = \dfrac{L_1 C_{p1}}{L_p - L_1} \end{cases} \tag{18}$$

In addition, according to the specified CC value and (14), the secondary compensation inducatance L_2 can be derived as

$$L_2 = \frac{2\sqrt{2}MU_{AB}}{\pi\omega_0 L_1 I_{Bat}} \tag{19}$$

In Figure 4(b), similarly, the secondary compensation capacitances C_{p2} and C_{f2} can be calculated according to the secondary resonant conditions

$$\begin{cases} C_{p2} = \dfrac{1}{\omega_0^2 L_2} \\ C_{f2} = \dfrac{L_1 C_{p2}}{L_s - L_2} \end{cases} \tag{20}$$

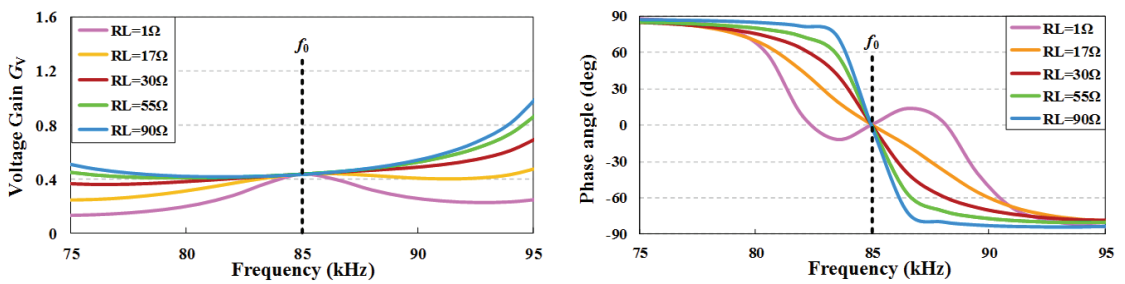

(a)

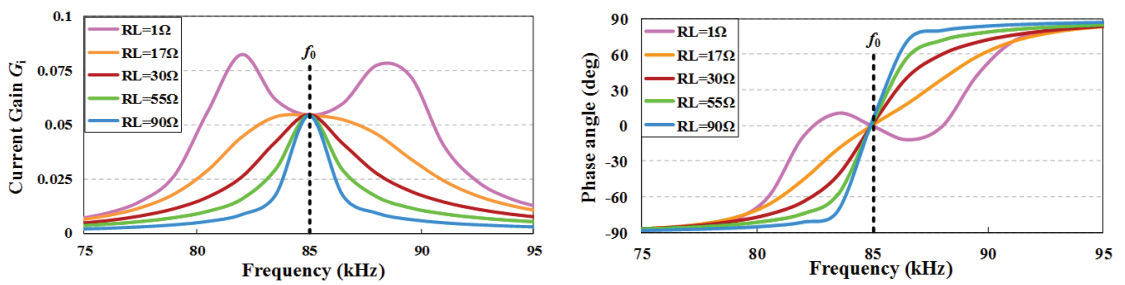

(b)

Fig. 5 Input phase angle and voltage/current gain of the proposed SHT
(a) for CV mode. (b) for CC mode.

In CV mode, according to the CV output condition, i.e., $\omega_0^2 = 1 / (MC_0)$, and by combining (4) and (5), the additional compensation capacitance C_1 can be derived as

Table 1. Specifications and parameters of the WPT system

Symbol	Quantity	Symbol	Quantity
U_{DC}	380 V	L_1	44.7 μH
ω_0	(2π × 85k) rad/s	L_2	12.5 μH
k	0.09	C_{p1}	78.5 nF
M	19.4 μH	C_{f1}	22.2 nF
L_p	203 μH	C_{p2}	280 nF
L_s	229 μH	C_{f2}	16.2 nF
C_1	140 nF		

$$C_1 = \frac{C_{f2}}{(L_s + L_2)\omega_0^2 C_{f2} - 1} \tag{21}$$

After the determination of LCT and the specification of CC and CV values, all the compensation devices of the proposed SHT can be determined according to (17)–(21). In this research, the charging current and voltage are designed to 20 A and 165 V, respectively. The designed system parameters are shown in Table 1. The input phase angle of the compensation topology is defined as

$$\theta_{\in} = \frac{180^{\circ}}{\pi} \tan \frac{\mathrm{Im}(Z_{\in})}{\mathrm{Re}(Z_{\in})} \tag{22}$$

where the operator "Im" represents the imaginary part, and "Re" represents the real part of the input impedance. The voltage gain G_V and current gain G_I of the proposed SHT are defined as follows:

$$\theta_{\in} = \frac{180^{\circ}}{\pi} \tan \frac{\mathrm{Im}(Z_{\in})}{\mathrm{Re}(Z_{\in})} \tag{23}$$

$$G_V = \frac{U_{ab}}{U_{AB}} = \frac{U_{Bat}}{U_{DC}} \tag{24}$$

$$G_I = \frac{I_{ab}}{U_{AB}} = \frac{I_{Bat}}{U_{DC}} \tag{25}$$

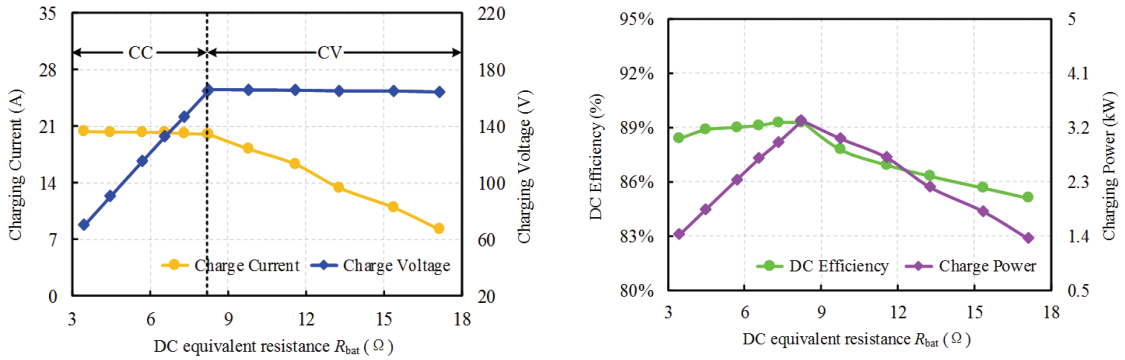

Fig. 6 Charging characteristics of the proposed hybrid charger.
(a) Measured charging profile; (b) Measured DC efficiency and charging power.

By using the designed parameters listed in Table 1, the voltage/current gain and phase angle of the porposed SHT are caluculated, as shown in Fig.5, the ZPA can be achieved at designed resonant frequency (85 kHz) both in CC mode and CV mode. In addition, the output voltage in CV mode and output current of CC mode both are constants at 85 kHz.

3. Experimental Verification

In order to verify the reasonability and feasibility of the proposed SHT-based WPT system, a 3.3-kW experimental WPT prototype is configured according to the parameters listed in Table 1. The deviation between the designed parameters and practical parameters is found to be less than 1%.

In this study, the specified values of I_{Bat} and U_{Bat} are designed to 20 A and 165 V, respectively. The charging characteristics of the proposed hybrid charger are shown in Fig. 6. In Fig.6 (a), it can be observed that as R_{Bat} increases, the charge current in CC mode and charge voltage in CV mode are almost constants. Measured DC efficiency and charge power are shown in Fig. 4(b); as the R_{Bat} increases, both DC efficiency andcharge power increase in CC mode and decrease in CV mode. The maximum DC efficiency (92.35%) and charge power (3.3 kW) are observed

The experimental waveforms are shown in Fig. 7. With the fluctuations of equivalent DC output resistance, charge current I_{Bat} in CC mode as well as the charge voltage U_{Bat} in CV mode are nearly constants. The plausibility of the proposed SHT is verified via the above experimental results.

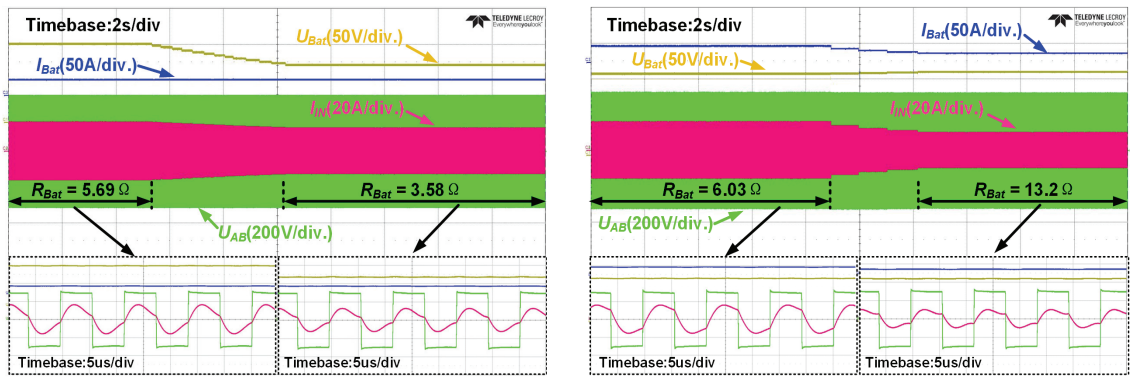

(a) (b)

Fig. 7 Experimental waveforms of CC and CV modes with load fluctuations.
(a) In CC mode (b) In CV mode

4. Conclusion

In this study, an SHT for EV wireless charging is proposed. The CC/CV charging and ZPA character can be implemented just via the switching between two ACSs. Due to the two ACSs are placed in primary side, the system can be easily controlled via only one primary controller and without synchronous wireless communication between transmitter and receiver. Thus, the cost and control complexity of the whole WPT system are significantly reduced. A 3.3-kW experimental prototype is configured to verify the charging performances of the proposed hybrid charger. The maximum DC efficiency (92.28%) and charge power (3.3 kW) are achieved at the critical charge point. The charging characteristics also remained stable during load fluctuation.

References

[1] S. Li and C. Mi, “Wireless power transfer for electric vehicle applications,” IEEE. J. Emerging Sel. Topics Power Electron., vol. 3, no. 1, pp. 4-17, Mar. 2015..

[2] Y. Jang and M. M. Jovanovic, “A contactless electrical energy transmission system for portable-telephone battery chargers,” IEEE Trans. Ind. Electron., vol. 50, no. 3, pp. 520-527, Jun. 2003.

[3] S. Liu, Z. Ye and W. Lu, “Electric vehicle dynamic wireless charging technology based on multi-parallel primary coils,” in Proc. 2018 IEEE Int. Conf. Electron. Comm. Eng. (ICECE), Dec 2018, pp. 120-124.

[4] C.-G. Kim, D.-H. Seo, J.-S. You, J.-H. Park, and B. H. Cho, ‘’Design of a contactless battery charger for cellular phone,’’ IEEE Trans. Ind. Electron., vol. 48, no. 6, pp. 1238-1247, Dec. 2001.

[5] X. Qu, H. Han, S.-C. Wong, C. K. Tse, and W. Chen, “Hybrid IPT topologies with constant current or constant voltage output for battery charging applications,” IEEE Trans. Power Electron., vol. 30, no. 11, pp. 6329-6337, Nov. 2015.

[6] S. Liu, Z. Ye and W. Lu, “Electric vehicle dynamic wireless charging technology based on multi-parallel primary coils,” in Proc. 2018 IEEE Int. Conf. Electron. Comm. Eng. (ICECE), Dec 2018, pp. 120-124.

[7] C.-G. Kim, D.-H. Seo, J.-S. You, J.-H. Park, and B. H. Cho, ‘’Design of a contactless battery charger for cellular phone,’’ IEEE Trans. Ind. Electron., vol. 48, no. 6, pp. 1238-1247, Dec. 2001.

[8] Z. Wang, X. Lai and Q. Wu, “A PSR CC/CV flyback converter with accurate CC control and optimized CV regulation strategy,” IEEE Trans. Power Electron., vol. 32, no. 9, pp. 7045-7055, Sep. 2017.

[9] H. N. Vu and W. J. Choi, “A novel dual full-bridge LLC resonant converter for CC and CV charges of batteries for electric vehicles,” IEEE Trans. Ind. Electron., vol. 65, no. 3, pp. 2212-2225, Mar. 2018.

[10] D. Ahn, S. Kim, J. Moon, and I. K. Cho, “Wireless power transfer with automatic feedback control of load resistance transformation,” IEEE Trans. Power Electron., vol. 31, no. 11, pp. 7876-7886, Nov. 2016.

[11] J. Byeon, M. Kang, M. Kim, D. Joo and B. Lee, “Hybrid control of inductive power transfer charger for electric vehicles using LCCL-S resonant network in limited operating frequency range,” in Proc. 2016 IEEE. ECCE, Sep 2018, pp. 978-984.

(Manuscript received February 25, 2020;
revised March 27, 2020; accepted April 3, 2020)